

**THE UNIVERSITY OF MICHIGAN
DEPARTMENT OF ATMOSPHERIC, OCEANIC, AND
SPACE SCIENCE**

**Space Physics Research Laboratory
2245 Hayward Street
Ann Arbor, Michigan 48109-2143**

Contract/Grant No.: NAG1-1720

Project Name: " Development of the Double
Etalon Fabry-Perot Interferometer
for Determining Total and
Tropospheric Ozone
Concentrations"

Report Author(s): William Cook

Author(s) Phone: (734) 763-5344

Report Preparation Date: 10/6/99

Report Type: Final Technical Report

Period Covered: 5/8/95-12/31/98

Project Director:
Principal Investigator(s): William Cook

Program Technical Officer:
Dr. Allen M. Larar
Mail Stop 401A
NASA Langley Research Center
Hampton, VA 23681-2199

Measuring and understanding the distribution of ozone through the lower levels of Earth's atmosphere are high priorities in global change and climate research. Of particular interest now is the global distribution of ozone in the upper troposphere and lower stratosphere. Global coverage of the stratospheric ozone is feasible only via remote sensing instruments on a space-based platform. And though extensive monitoring tropospheric ozone is possible using instruments flown aboard conventional aircraft, a space-based system would be significantly less costly and provide information over a much broader area and produce more uniform coverage.

Here we describe the prototype of an instrument being developed to monitor, from an orbiting spacecraft, the ozone found in Earth's upper troposphere and lower stratosphere. Our new spectrometer is an infrared Fabry-Perot interferometer which uses two synchronously tuned etalons: a high resolution narrow band device and a lower resolution broader band filtering etalon. The prototype is a scanning device making use of nearly collimated input radiation and a single element detector. As presently configured, it is capable of providing a resolution better than 0.07 cm^{-1} with a spectral band width approximately 5 cm^{-1} wide and centered at 1054.7 cm^{-1} .

For the future space-based emission device a modification of the the prototype was to be made to employ innovative circle-to-line detector optics, those developed or in development at UM/SPRL, and a focal plane array detector. These enhancements would enable a simultaneous recording of the entire spectral range of interest, but with simple detection electronics and a significant gain in signal-to-noise over that of the scanning version.

1.0 Introduction

Ozone is one of the most important trace gases in Earth's atmosphere, playing a role in global climate change and atmospheric pollution mechanisms. Stratospheric ozone plays an important role in sustaining life on the surface as it screens out most of the harmful ultraviolet radiation reaching Earth from the Sun. However, when present in the lower troposphere ozone acts as a pollutant since it is highly toxic to both plants and animals. Ozone is a "greenhouse gas" and plays a significant role in the warming of the middle stratosphere. Recent work suggests that increasing tropospheric ozone could produce an effect comparable to the changes expected from increased global CO_2 concentrations.

Studies of the chemistry of ozone production are providing a clearer picture of the various mechanisms by which ozone can be produced or destroyed in particular regions of the atmosphere. Photochemistry involving chlorine and OH radicals plays a major role in destroying ozone in the stratosphere, while nitrogen oxide compounds and hydrocarbons seem to be the major components involved in tropospheric ozone chemistry. Great strides have been made in understanding the various mechanisms of stratospheric ozone loss, but current models do not describe the ozone content of the lower stratosphere very well. Work to improve the models is hampered by incomplete knowledge of the global distribution of ozone in the lower stratosphere. Since it is likely that there is some coupling between the lower stratosphere and the troposphere, a complete understanding of the ozone dynamics will also require measurement of upper tropospheric ozone on a global basis.

Surface ozone is of concern as it is a very toxic pollutant. Ozone is known to cause many human respiratory problems associated with urban smog. It has been linked to significant damage in plants such as food crops and natural forests, thus producing a negative effect on human economic activity. The origins of tropospheric ozone or its precursors are both anthropogenic and natural including : industrial and agricultural by-products, auto emissions, biogenic emissions, lightning and stratospheric-tropospheric exchange. Understanding tropospheric ozone transport on

regional or larger scales requires that the global distribution of both tropospheric and stratospheric ozone be monitored with fairly high spatial and temporal resolution.

Because ozone has been identified as a key component in our environment and changes in ozone distribution are likely to have important consequences in regard to global climate, world leaders are recognizing the need to further understand and perhaps regulate processes involved in ozone production and destruction. Several important studies have led the scientific community to conclude that understanding the global distribution of ozone in the troposphere and stratosphere is a major priority.

2.0 Description of the Prototype Double Etalon Spectrometer

Details of the operation of Fabry-Perot interferometers will not be given here. Readers unfamiliar with the device should refer to standard optics texts. Additional details specific to the double etalon FPI are given in Larar, 1993.

The optical portion of the instrument was mounted on a vibration resistant optical table on the second floor of the Space Physics Research Building on campus at the U. of Michigan. Most of the electronics used were mounted on a rack near the table, and the computers on a table nearby. The hardware comprising the sun-tacker was mounted on the roof of the building, with a non-domed opening allowing direct incidence of the sunlight onto the table optics.

Two Fabry-Perot etalons form the dispersive element central to the spectrometer described in this report. However, to ensure that the spectral information collected from these etalons is meaningful, three additional subsystems are employed that either actively ensure the quality of the spectral data or provide information regarding the quality of the acquired spectral data. These additional subsystems include an active feedback system used to maintain alignment of the etalons and to accurately control their spacings, a computer controlled system used to maintain accurate pointing of the sun-tracking device, and a broadband photometer used to identify contamination of the spectral data by clouds. Hence, the instrument described herein can be conveniently broken into four interdependent subsystems.

The primary subsystem of this instrument is the infrared spectrometer shown in the schematic Figure 1, of which the two Fabry-Perot etalons are the main components. However, another essential segment of this first subsystem are the collimating foreoptics. The collimating foreoptics are composed of two sets of 3 mirrors, coupled with a 4~mm diameter aperture. Of these six mirrors those labeled "m" in Figure 1 are flat, included in the system only to direct the sunlight onto the aperture and into the etalons. The mirrors labeled "s1" are both f/20 converging mirrors that together with the aperture collimate the light. These collimating optics also limit the instrument field of view to 1/4 degree since the area of the solar image that is formed on the 12.6~mm² aperture is 8 mm². The final collimated beam is 50 mm in diameter, coinciding with the diameters of the converging foreoptics mirrors.

The etalons are the second and main components of this subsystem. Each etalon consists of two ZnSe substrates that exhibit random surface imperfections of approximately $\lambda/100$ at 633 nm. A dielectric coating that is 91 percent reflective at 9.5 μ m wavelength covers the inner 45~mm diameter of these substrates. This same coating has a reflectance of approximately 30 percent at the alignment laser wavelength of 633 nm. The high resolution etalon is the first in the pair, having a nominal spacing of 0.340 cm between its reflecting surfaces. This etalon is followed by an aluminum coated mirror, placed between the etalons primarily to provide a 'lossy' medium for improved system contrast. However, a second function of this mirror is to direct the solar radiation into the low resolution etalon. The low resolution etalon is identical to

the high resolution etalon except that it is configured for a nominal 0.095 cm separation between the etalon plates. These plate spacings were carefully chosen, as will be explained below.

The final segment of this subsystem are the fringe-forming optics, a narrowband filter, and the detector. In Figure 1, the mirror labeled "s2" is an f/6 converging mirror. These mirrors are also 50 mm in diameter. The objective mirror produces an image of the sun on the detector that is slightly more than 1.5 mm in diameter, overfilling the area of the detector cathode (1 mm²). The narrowband filter is placed immediately before the detector and is centered at a wavelength of 1055 cm⁻¹ with a full-width at half-maximum of approximately 6 cm⁻¹. It was specially manufactured by Optical Coatings Laboratory Incorporated (OCLI) for this project. The filter was wedged to eliminate channeling of the spectra, and the wedge angle produced a 22-degree refraction in the beam direction. As will be discussed in greater detail shortly, the full-width at half-maximum (FWHM) of this filter is approximately equal to the free spectral range of the low resolution etalon. However, the FWHM is approximately one half of the combined dual-etalon passband. As such, only one order of the solar spectra is observed at any time.

The detector used in this version of the instrument is a single element, liquid nitrogen cooled, MCT (Mercury Cadmium Telluride) detector from EG&G Judson. This detector is sensitive to IR radiation with wavelengths longer than 8 μ m. The OCLI filter is extreme narrow, centered at 1055 cm⁻¹, but allows a detectable amount of long wave radiation through. Hence, a second filter composed of CaF₂ was inserted into the optical path immediately following the aperture used in collimating the sunlight (aperture A1). The addition of this filter eliminates unwanted radiation that would otherwise pass through the windows of the OCLI filter.

A secondary subsystem utilizing a low-power frequency-stabilized HeNe laser maintains the alignment of the etalons, both singly and collectively, throughout an entire experiment. That is, this alignment subsystem maintains the parallelism of each set of etalon plates and the nominal spacing within the cavities of the etalons. This is done by monitoring a designated order of the HeNe spectra throughout an entire experiment, thus enabling the instrument to behave in a fashion that is repeatable from one measure of the solar spectra to the next. This automation is important as a single experiment can last in excess of 10 hours when multiple data sets are obtained.

The HeNe laser beam used for this alignment is first expanded to a diameter of approximately 20 mm before entering the etalons. This is done so that information from a large finite segment of the etalon plates will be encoded onto the HeNe beam. Additional expansion of the beam beyond this size proved to offer no benefit, and keeping the beam diameter small allowed the use of smaller secondary optics. Thus, only this finite segment of the etalon plates transmits the 633 nm wavelength at any time. The expansion of the laser beam is accomplished using the telescope and various flat mirrors not shown in the figure. The beam is directed into the etalons using a ZnSe beam splitter located at the position of the mirror labeled "mr" in Figure 1. The ZnSe material was chosen because this beam splitter must be transparent to 9.5 μ m radiation while being reflective (enough) of the HeNe light. Other materials are also suitable, but the ZnSe window was already available to us. Although most of the HeNe beam also passes through this beam splitter, a sufficient amount enters the etalons and is eventually brought to a focus at aperture "a" using the previously described foreoptics. To gain access to the information contained in the laser beam a broadband IR filter, that is 85 percent transmitting at 9.5 μ m yet highly reflective in the visible, is placed at the position of the aperture between the aperture and the chopper blade "ch". This filter reflects the laser light onto a photodiode for detection. Further, this broadband IR filter blocks all visible sunlight that would otherwise pass through aperture and saturate the

photodiode detector used to detect the laser. It has the added benefit of blocking UV radiation that would otherwise degrade the ZnSe etalon substrates and coatings.

This alignment subsystem uses only one detector to align two etalons. Hence, the etalons must be aligned sequentially. The algorithm used to align each etalon works to maximize the intensity of the HeNe beam at the photodiode detector. This is done using a “random walk” procedure wherein the piezoelectric elements (PZT’s) controlling the etalon alignment are perturbed about their current positions until a maximum in the detected intensity is found. There are 3 PZT’s mounted on one plate in each etalon, spaced uniformly around the outside of the plate by the manufacturer (Burleigh Instruments). Controllers designed and tuned for these elements were used, manually to initiate alignment and then automatically under computer control to improve and maintain alignment. The PZT’s were also used to change the etalon spacings as will be described in more detail below.

There are thirteen separate adjustments that can be made to an etalon containing three PZTs. These include adjusting one PZT while holding the others fixed and adjusting two or three PZTs simultaneously in the same or opposite directions. An adjustment of all three simultaneously in the same direction has the effect of changing the wavelength on which the etalon passband is centered. Each alignment of an etalon begins with an adjustment of all three pzt’s simultaneously until the etalon passband is centered upon the peak of a chosen HeNe fringe. This order of the HeNe fringe pattern remains the same throughout the duration of an experiment. Though seemingly complicated, the process can acquire and maintain alignment within about one second of its initiation.

The final optical subsystem of this instrument is an IR photometer. The purpose of this photometer is to identify periods of cloud cover, that may have corrupted the spectral data. This photometer measures radiation across a 200 cm^{-1} band centered at about $9.5\text{ }\mu\text{m}$. It uses the beam reflected off the first surface of one of the ZnSe substrates that make up the high resolution etalon. This reflected beam returns slightly off-center from aperture A1 due to the 3 arc second wedge angle in the etalon substrates. This reflected beam is directed onto a second MCT detector by two small folding mirrors placed near aperture A1. Thus a radiometric-type measurement is also acquired during the high-resolution scan. This allows the detection of large changes in intensity which could occur due to (visibly) invisible water vapor clouds drifting into or out of the instrument’s field of view. Hence “bad” datasets are directly indicated by the radiometer data.

The electronic interface between the user and the optics provides full automation of this instrument by establishing 1) electronic control of the 6 piezoelectric stacks in the etalons, 2) the ability to acquire detector output, and 3) electronic control of the sun-tracking device. Two RG-93 etalon controllers from Burleigh Corporation, coupled with eight 12-bit D/A channels provide PC control over the settings of the individual piezoelectric stacks that adjust the etalons. Two separate lock-in amplifiers provide detection of the signals from the two MCT detectors serving the IR spectrometer and the IR photometer. A third lock-in amplifier provides detection of the signal from the photodiode detector serving the etalon alignment subsystem. Information is passed from the lock-in amplifiers to the PC over RS232 serial lines in the case of the two lock-in amplifiers connected to the IR detectors. The output signal from the lock-in amplifier connected to the photodiode detector is sampled using a 12-bit A/D channel. The sun-tracking device is controlled using a second PC that is connected to a PMG200-P dual-axis motion controller from Newport via a RS232 serial connection. The motion controller adjusts the declination and azimuth of the sun-tracking device using two motorized rotation stages. All control software is written in

Fortran, linked with Assembly language interfaces controlling the various serial, D/A, and A/D ports.

3.0 Operation and Results

The spectrometer in this prototype instrument utilizes a single-element detector. Thus, it is only possible to examine a very small subregion of the full spectra at any given time. Consequently, the spectra must be scanned, in time, across the detector to build up a measure of the full spectral region. Shown in Figure 2 is a comparison of the OCLI filter passband with the theoretical instrument functions (and corresponding free spectral ranges) of the high and low resolution etalons. As is evident, the filter has a finite transmission over a spectral region that is approximately 1.5 times wider than the free spectral range of the low resolution etalon and approximately .5 times wider than the free spectral range of the high resolution etalon. Thus, if data is to be collected across the full bandpass of the OCLI filter, it is necessary to scan the etalons through multiple orders of their respective free spectral ranges.

The etalon passbands are scanned by mechanically adjusting the spacing within the etalon cavities. This mechanical adjustment is accomplished using piezoelectric elements that provide approximately 6-micron of movement. This 6 μm motion allows the etalons to be scanned through approximately 1.3 of their respective free spectral ranges. This amount is sufficient to scan the low resolution etalon across most of the OCLI filter bandpass. However, it is not sufficient to do the same with the high resolution etalon. Hence, an alternative approach to collecting data must be employed that allows the full bandpass of the OCLI filter to be scanned, yet only requires the high resolution etalon be scanned through at most 1.3 free spectral ranges.

This approach utilizes the different orders of the high resolution etalon to obtain a spectral measurement over the full bandpass of the OCLI filter. That is, a scan of the full spectral region is divided into a series of 5 subscans. During each subscan the low resolution etalon passband is scanned along with a specifically chosen order of the high resolution etalon. For example, orders L1 and H1 may be scanned together. After the high resolution etalon has been scanned its full amount (approximately 1.3 free spectral ranges) it is reset and the process is repeated with the low resolution etalon now scanned synchronously with the next higher order of the high resolution etalon. That is, L1 and H2 are subsequently scanned together. Thus, rather than scan one single order of the high resolution etalon through the entire filter passband, the low resolution etalon hops from one order of the high resolution etalon to the next. In this way, a spectral measurement over the full filter bandpass is achieved by 'ratcheting' the scan of the high resolution etalon.

The performance of a spectrometer is well described by the combination of instrument sensitivity and spectral resolution. As this prototype instrument was designed for solar absorption measurements made from a ground-based platform, the demands upon sensitivity are reduced somewhat below that of the subsequent emission instrument. However, the required resolution of 0.07 cm^{-1} in the 1055 cm^{-1} region of the solar spectrum is set by the need to discriminate between tropospheric and stratospheric ozone based upon line shape. This requirement is the same for the prototype and the forthcoming emission instrument.

The resolution of a dual-etalon Fabry-Perot interferometer depends largely upon the reflectance of the etalon coatings and the spacing within the cavity of the high resolution etalon.

The reflectance of the coatings defines a quantity known as the reflectivity finesse and the spacing of the etalon cavity sets the free spectral range of the high resolution etalon. The quotient of these two gives the resolution of a perfect etalon. The etalons used in this instrument have a coating that is 90 percent reflective at a wavelength of $9.5\text{ }\mu\text{m}$ which was independently verified

through measurements made on our Bruker IFS66 spectrometer. The corresponding reflective finesse is approximately 30. The spacing of the high resolution etalon is 0.340 cm and hence the free spectral range of this etalon is 1.5 cm^{-1} . Thus, if this were a perfect Fabry-Perot etalon, the achieved resolution would be expected to be better than 0.05 cm^{-1} . As with all Fabry-Perot etalons, however, those used in this instrument are not perfect but could exhibit defects that reduce the achieved spectral resolution below that of a perfect etalon. The three primary defects are 1) random surface imperfections in the etalon plates, 2) a spherical curvature (or bowing) in the etalon plates produced by an imperfect mounting system, and 3) error in the achieved parallelism of the etalon plates. Each of these imperfections can be characterized by an associated 'defect' finesse.

The good surface quality of the plates made negligible any contributions to reduced finesse due to "defects". Calculation of potential degradation in finesse due to the other two factors is difficult, so a measurement of the finesses of the two etalons was performed. Using a blackbody source and "fixed" values for plate spacings of the unmeasured etalon, the finesse of both the high and low resolution etalons was found to be between 25 and 30 – or very nearly that due to the reflectivity alone. This indicates that both the errors in parallelism and the spherical deformities were well within tolerable limits. The "design" finesse for the instrument was 15, and we far exceeded this. Hence our achieved spectral resolution was also better than the anticipated 0.07 cm^{-1} .

Solar absorption spectra have been measured from the campus of the University of Michigan in Ann Arbor using the prototype instrument described above. The best observations were made on nine dates beginning September 18, 1997 and ending October 10, 1997. An example of these spectra is shown in Figure 3, uncorrected for signal background. Obvious absorption features are seen in these data and these absorption features are easily recognized when compared with the predictions shown in this same figure. It should be noted, however, that the spectra can be corrected using a simple linear fit (Larar, 1998) to match very closely a standard absorption prediction. The theoretical curve shown in Figure 4 was not "fit" to the data, but was calculated from "typical" values for the time of year and solar zenith angle of the scan. It is seen that the achieved resolution is indeed high and the measurements resolve even the closest spectral features.

The stability of this instrument on time scales of minutes is shown by the regions of overlap within a given spectra. This overlap is an intentional part of the data-collection routine described earlier wherein a measure of the entire spectral region is divided into five separate subregions and each subregion corresponds to a full scan of the high resolution etalon. With each reset of the etalons, a small spectral region of overlap is obtained. It is seen here that the signal level measured just after the reset occurs is nearly identical to that measured just prior to the reset. Hence, the hysteresis that accompanies the motion of the pzts with each reset does not significantly degrade the system performance.

The spectra shown in the figures below were sampled using approximately 400 channels and each required roughly 10~minutes to collect. To withdraw estimates of tropospheric ozone density from measurements of this spectral region it is not necessary to use so many points in the sampling process. However, the motivation behind these measurements is to demonstrate the capabilities of the instrument (in part by an unambiguous identification of the solar spectra) and as such these spectra were purposely oversampled. Given that each spectra required approximately 10~minutes to acquire it is possible that the atmospheric transparency along the line-of-sight of the instrument may have varied during this time. This possibility can be tested by examining the

data collected simultaneously by the broadband photometer described earlier. The photometer data corresponding to the spectrum in Figure 4 is shown in Figure 5 and indicates that the transparency of the atmosphere did not vary significantly while the solar spectra were acquired.

The instrument, configured for single-element detector operation, clearly demonstrates the capability of a double-etalon IR device used as a ground-based spectrometer for the measurement of ozone. Critical subsystems, the etalon spacing and alignment controls, were developed and proven to work. It was also shown that plates of sufficient (indeed nearly ideal) optical quality could be produced and mounted with no significant finesse-reducing strain. Operational software was produced for the system.

A second goal of the project, the introduction of the Circle-to-Line Interferometer Optics (CLIO) was also begun. The complete design and expected results (incorporated in a report by G. Lindquist) were submitted as part of an interim report. The last several months of the project concentrated on implementing this design, which required a complete re-configuration of the spectrometer and introduction of new fore and focusing optics. Difficulty immediately arose in that the planned for focal plane array detector never became available, this was due both to budgetary and technical shortfalls. We attempted to simulate a 2-dimensional detector by mounting our single element detector on a translation stage. The axes of the stage were controlled via computer and it was possible to precisely position the detector anywhere within the illuminated portion of the focal plane. Unfortunately, obtaining complete images of the focal plane was very time consuming, which (combined with the peculiar nature of the image formed by the off-axis CLIO and the "kink" introduced into the beam direction by the wedged filter) ultimately made alignment of the spectrometer impossible. Numerous images were acquired and various strategies employed to align the system. None proved capable of aligning and holding alignment through a spectral scan.

Publications citing NASA LaRC support for this work:

A.M. Larar, W.B. Cook, and R.S. Lancaster, "Laboratory Prototype Double-Etalon Fabry-Perot Interferometer for Remotely Sensing Atmospheric Ozone: Atmospheric Measurements," in *Infrared Spaceborne Remote Sensing VI*, M. Scholl, editor, Proc. of SPIE 3437, 158-166 (1998).

A. M. Larar, P. M. Sandford, W. B. Cook, J. M. Reeves, P. B. Hays, J. J. Puschell and D. H. Ceckowski, "Tropospheric ozone sensing Fabry-Perot interferometer: recent laboratory advancements", in *Optical Spectroscopic Techniques and Instrumentation for Atmospheric and Space Research II*, Jinxue Wang and Paul B. Hays, Editors, Proc. SPIE 2830, 127-134 (1996).

William B. Cook, Redgie S. Lancaster and Allen. M. Larar, "Laboratory Prototype Double-Etalon Fabry-Perot Interferometer for Remotely Sensing Atmospheric Ozone: Hardware Configuration" at the *Infrared Spaceborne Remote Sensing VI*, SPIE conference, San Diego, CA, July 1998.

Manuscript in preparation for Applied Optics, authors W. B. Cook, R. Lancaster, A. M. Larar, G. Lindquist, and M. Reeves

Students supported:

J. Michael Reeves (post-doctoral fellow) 1995-1996

Redgie Lancaster (post-doctoral fellow) 1997-1998

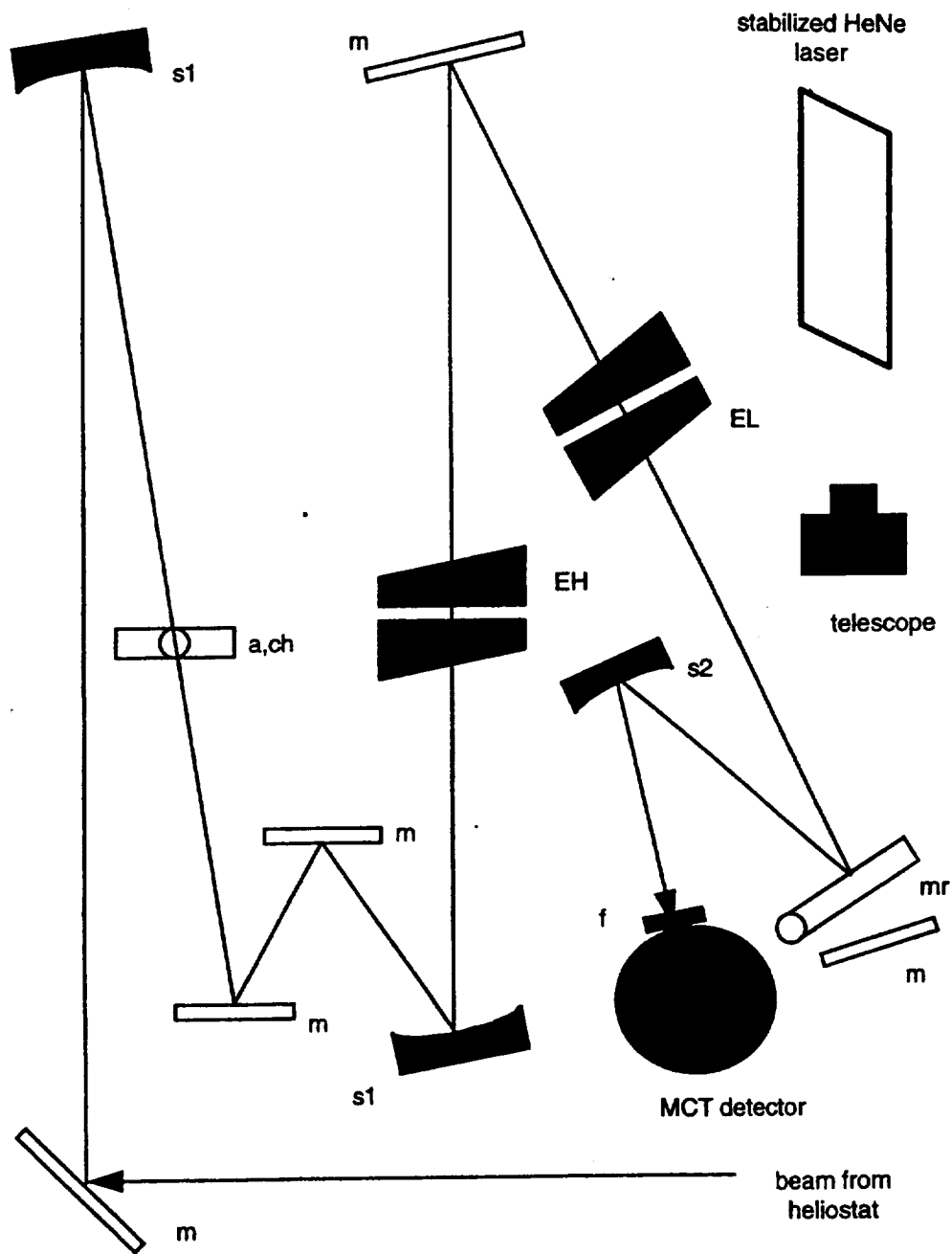


Figure 1. Schematic diagram of the laboratory prototype double etalon spectrometer showing: plane mirrors (m); aperture (a); chopper blade (ch); 100cm focal length spherical mirrors for beam collimation (s1); high resolution etalon (EH); low resolution etalon (EL); a mirror mounted to allow its easy removal for HeNe alignment (mr); a 25cm focal length focusing mirror (s2); narrow bandpass filter (f); the MCT detector; and the HeNe alignment laser system.

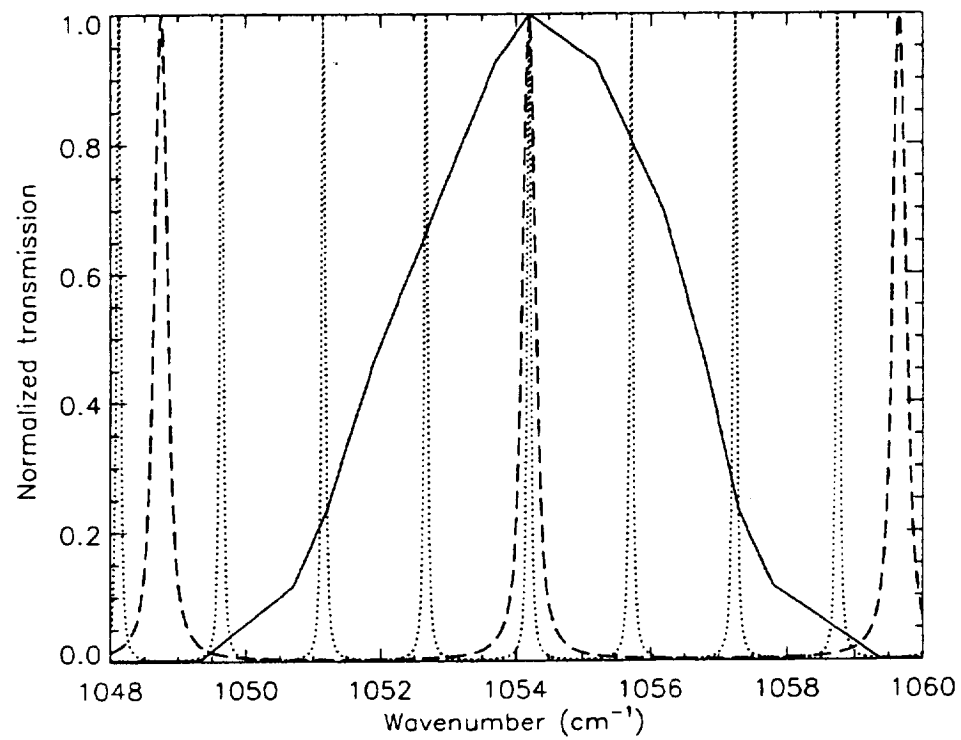


Figure 2. Instrument transfer functions: measured bandpass filter curve (as provided by OCLI) (solid) and our calculated etalon transmission functions for the HRE (dotted) and LRE (dashed) functions (ignoring plate imperfections).

**2XE solar spectrum
about 1 hour past local noon**

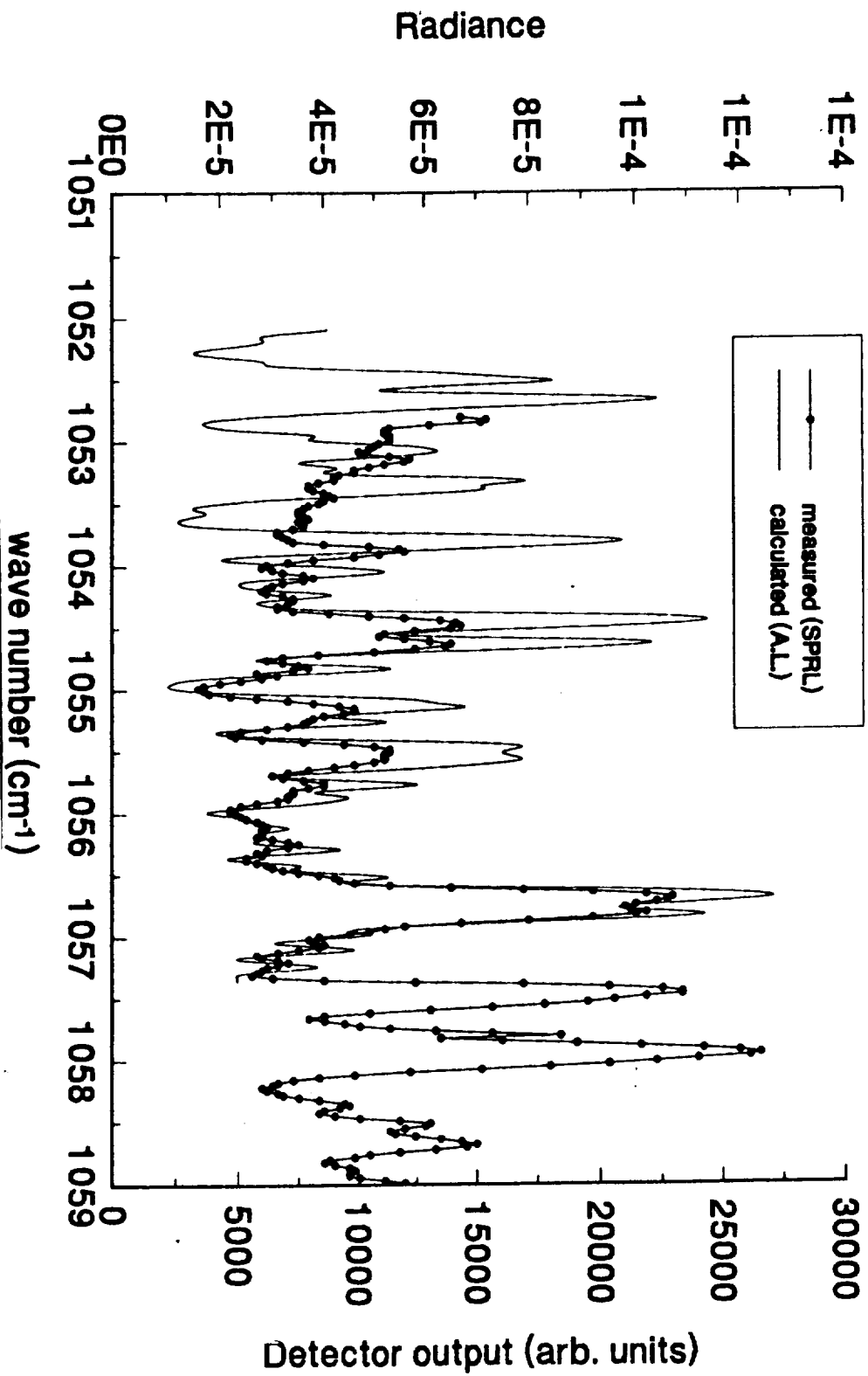


Figure 3.

FPI sunlook test: sep2497, szo=44.

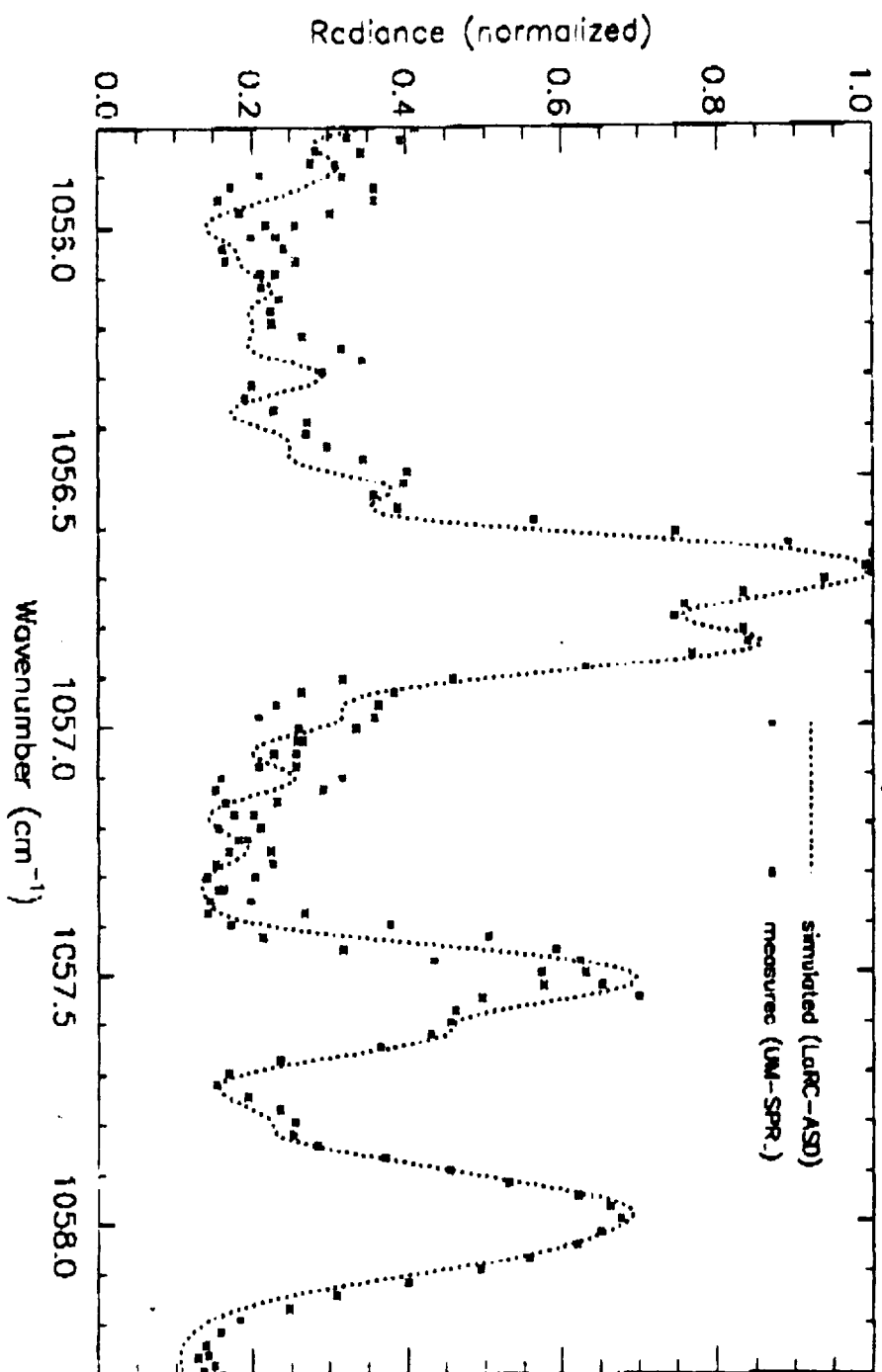


Figure 4.

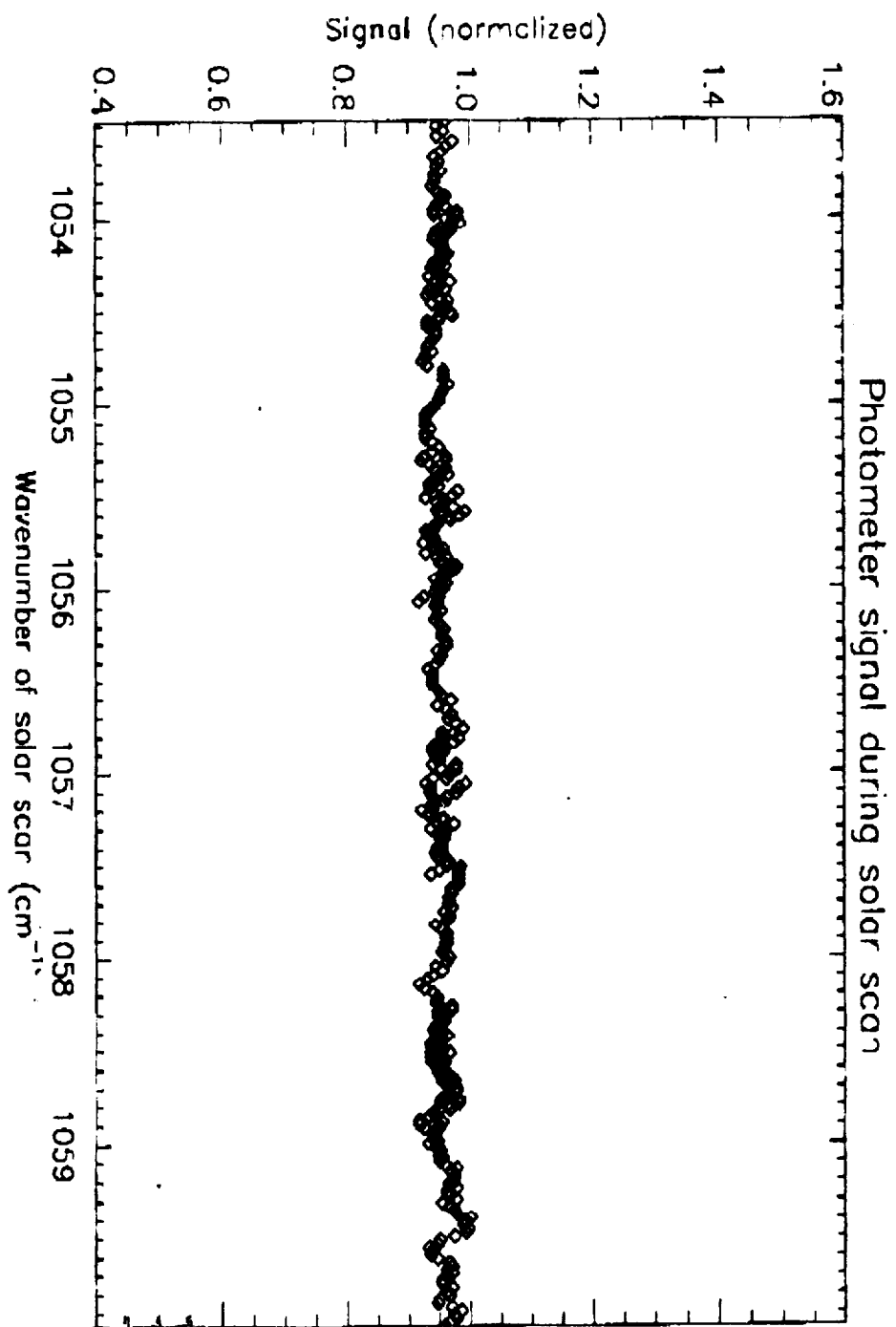


Figure 5.



UNIVERSITY OF MICHIGAN
COLLEGE OF ENGINEERING
ATMOSPHERIC, OCEANIC AND SPACE SCIENCES

SPACE RESEARCH BUILDING
2455 HAYWARD
ANN ARBOR, MICHIGAN 48109-2143
TELEPHONE: 734 764-3335 FAX: 734 764-4585

6 October 1999

Dr. Allen M. Larar
Mail Stop 401A
NASA Langley Research Center
Hampton, VA 23681-2199

Subject: Final Technical Report Grant NAG1-1720

Dear Dr. Larar,

On behalf of William Cook, the project director, and in compliance with the requirements of the Grant NAG1-1720 entitled "Development of the Double Etalon Fabry-Perot Interferometer for Determining Total and Tropospheric Ozone Concentrations", I am forwarding the enclosed final technical report.

If you have any questions or need additional information please contact William Cook at (734) 763-5344.

Sincerely,

A handwritten signature in cursive script that reads "Cheri Hovater".

Cheri Hovater
Administrative Assistant

ch

encls.

cc: CASI
Grants Office MS 126
W.Cook
ONR/Chicago w/o encls.
N.Gerl w/o encls.
file 033245